Electronic Supplementary Material (ESI) for Journal of Materials Chemistry A.
This journal is © The Royal Society of Chemistry 2018

# Supporting Information

# A separator-based lithium polysulfides recirculator for high-loading and high-performance Li-S batteries

**Ming Li,‡[a] Chao Wang,‡[b,c*] Lixiao Miao,[d] Jingwei Xiang,[a] Tanyuan Wang,[a] Kai Yuan,[a] Jitao Chen,[e*] Yunhui Huang[a,b*]**

[a] State Key Laboratory of Materials Processing and Die & Mould Technology, School of Materials Science and Engineering, Huazhong University of Science and Technology, Wuhan, Hubei 430074, PR China.

[b] Institute of New Energy for Vehicles; School of Materials Science and Engineering, Tongji University, Shanghai 201804, PR China.

[c] Department of Nuclear Science and Engineering, Massachusetts Institute of Technology, Cambridge, Massachusetts 02139, USA.

[d] Sound Group Institute of New Energy, Beijing, PR China.

[e] College of Chemistry and Molecular Engineering, Peking University, Beijing, PR China.

‡ Chao Wang and Ming Li contributed equally to this work.

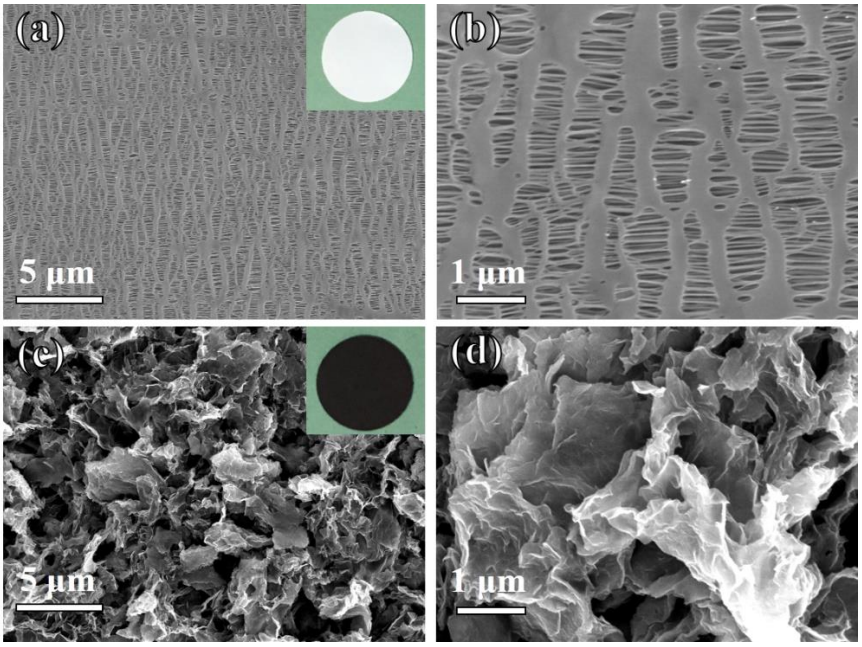


**Fig. S1** (a) (b) The digital photo and SEM images of Celgard separator. (c) (d) The digital photo and SEM images of MoP/rGO modified separator.

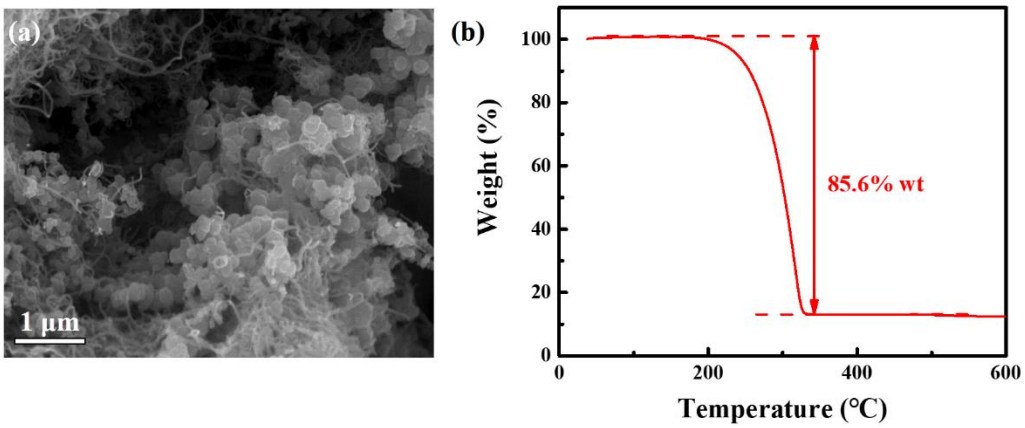


**Fig. S2** (a) The SEM image of S/C composites. (b) The TGA curve of S/C composites under Ar atmosphere.

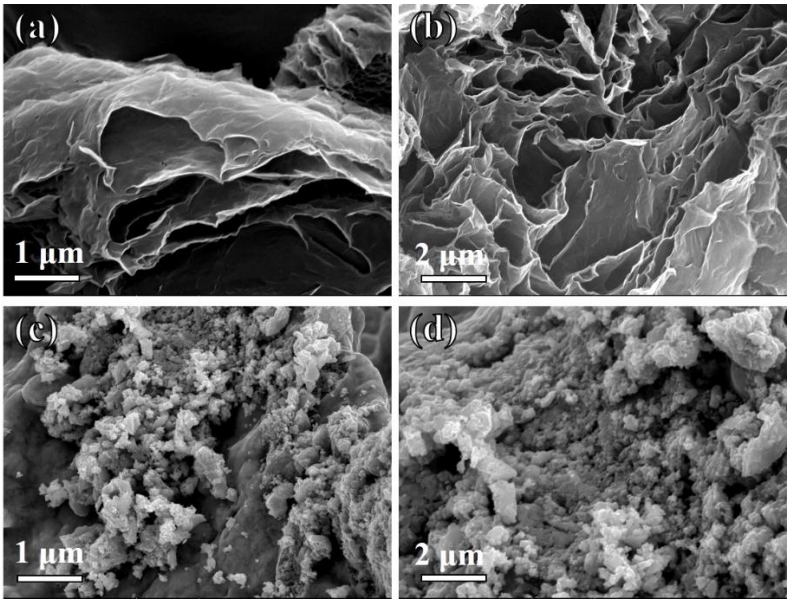


**Fig. S3** (a) (b) The SEM images of pure rGO. (c) (d) The SEM images of bulk MoP.

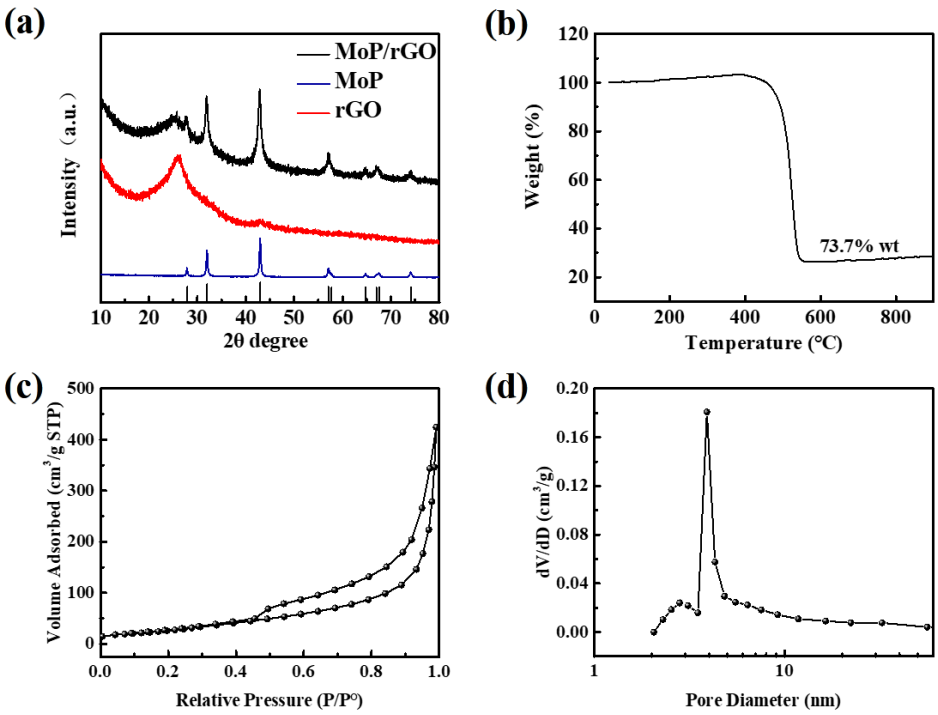


**Fig. S4** (a) XRD patterns of MoP/rGO, rGO and MoP. (b) TGA curve of MoP/rGO composites under air atmosphere (the final product is $MoO_3$). (c) $N_2$ adsorption-desorption isotherms of MoP/rGO composites. (d) The pore size distribution of the MoP/rGO composites.

To confirm the rGO content of the composites, the TGA measurement was made at 0~600 $^{o}$C under air atomosphere. The final product of MoP/rGO composites was $MoO_3$. From the TGA results, the mass of $MoO_3$ was about 26.3 % of the total mass.

So the content of MoP in initial composites was 26.3 % * 127/144 = 23.2 % (the relative molecular mass of MoP and $MoO_3$ are 127 and 144, respectively), which means the rGO content of the composites was about 76.8 %.

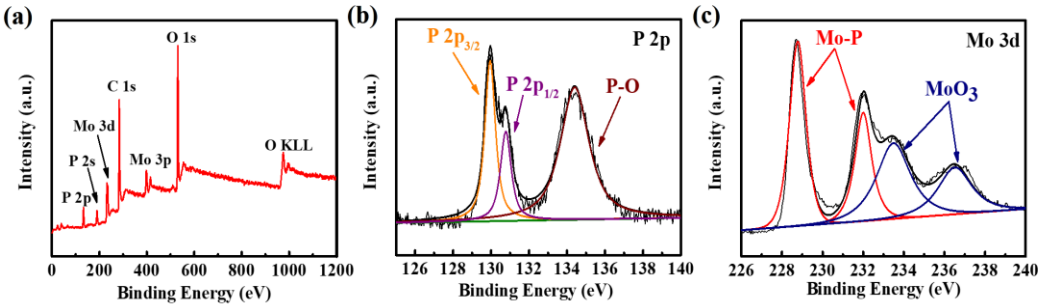


**Fig. S5** (a) wide-scan, (b) P 2p and (c) Mo 3d XPS spectra of MoP/rGO composites.

## Polysulfides Adsorption Experiment

The $Li_2S_6$ solution was prepared as follows. $S_8$ and $Li_2S$ were dissolved in 1, 3-dioxolane (DOL) and 1, 2-dimethoxyethane (DME) (1:1 by volume) with a molar ratio of 5:8. Then the mixture was stirred at 60 °C for 24 h in Argon-filled glovebox. The concentration of the obtained $Li_2S_6$ solution was 1 mg $mL^{-1}$. An equivalent amount (10 mg) of different polysulfide host materials (MoP/rGO, rGO and bulk MoP for comparison) were immersed into a 2 mL $Li_2S_6$ solution and held for 2 h.

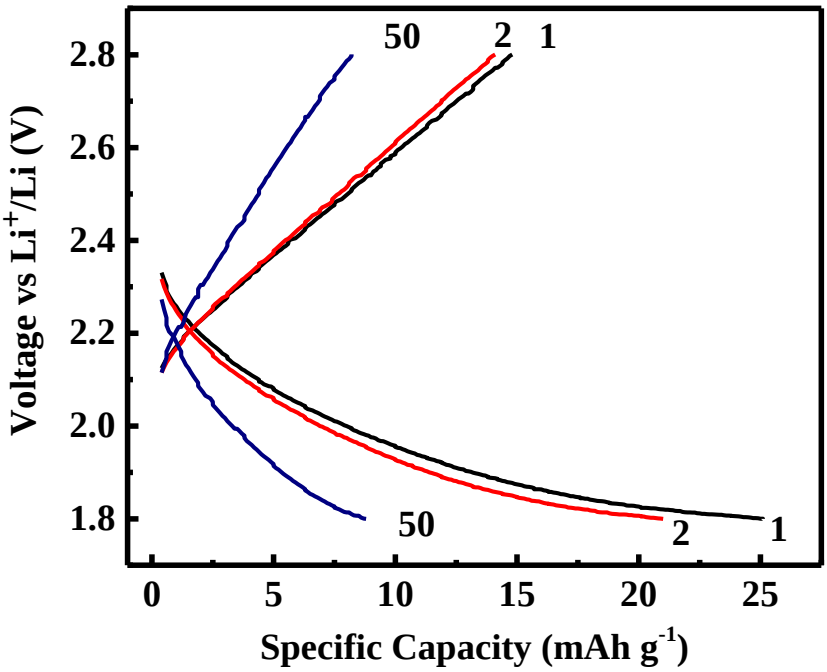


**Fig. S6** Different cycles of galvanostatic discharge-charge curves of MoP/rGO composite between 1.8 and 2.8 V at 0.5 C.

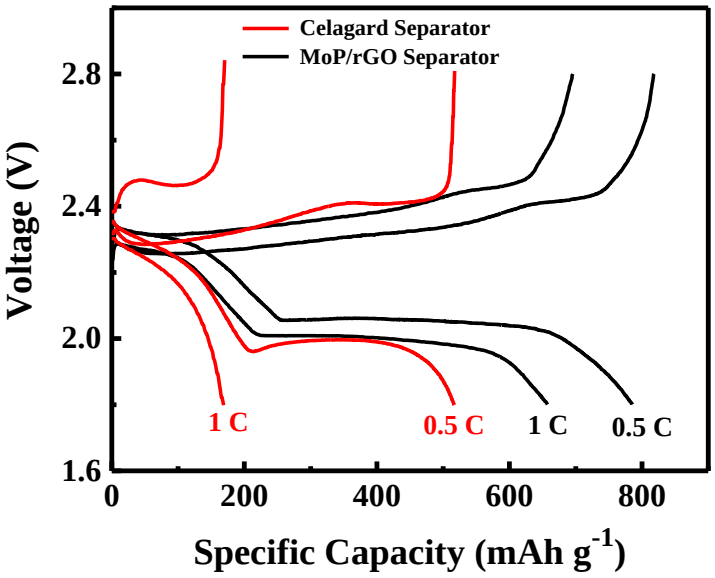


**Fig. S7** Galvanostatic discharge-charge profiles of cells with different separators at rate of 0.1C and 0.5C.

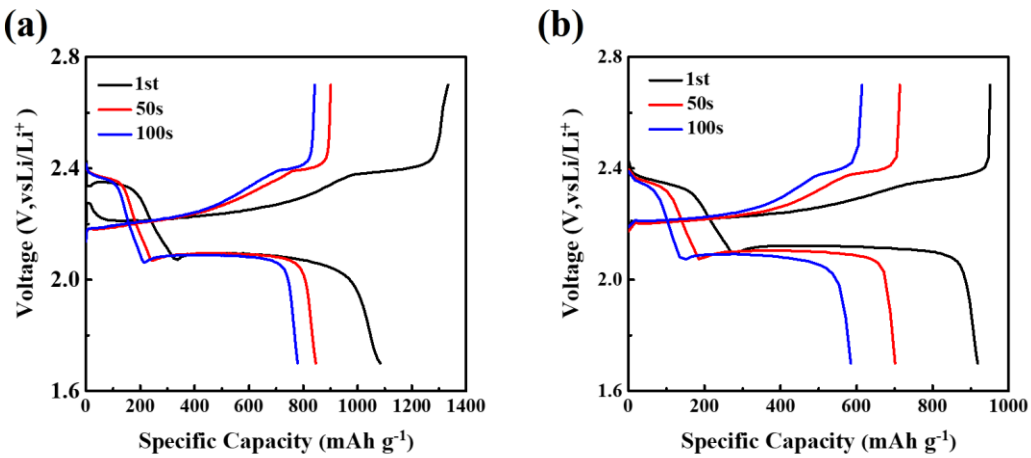


**Fig. S8** Galvanostatic discharge-charge profiles of pouch cells with (a) MoP/rGO modified separator, (b) Celgard separator separators at different cycles.

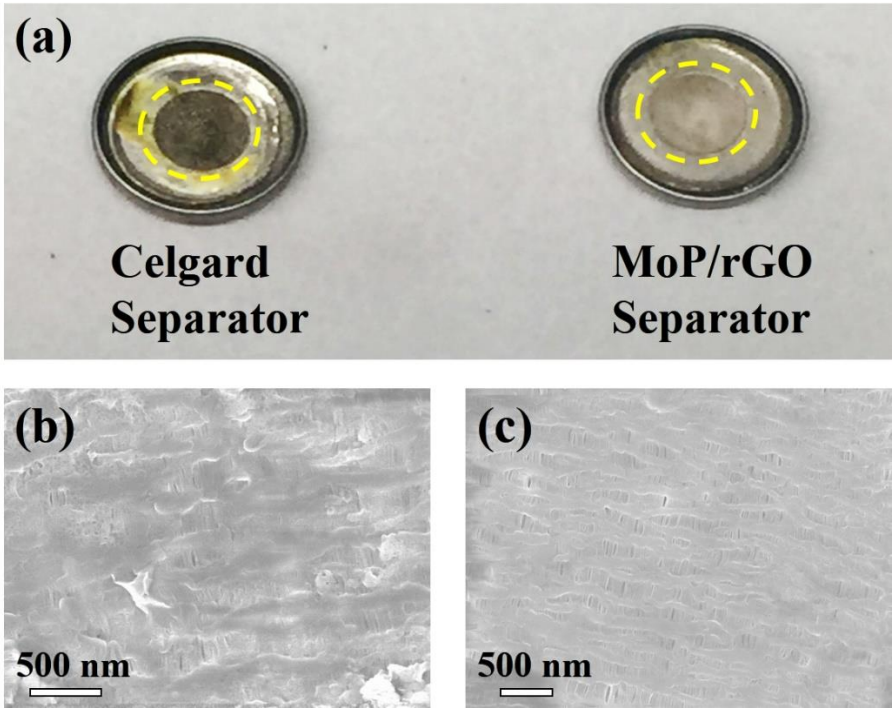


**Fig. S9** (a) Photograph of lithium anodes in cells with different separators after cycling. (b) (c) SEM images of the surface faced to the lithium anode of Celgard and MoP/rGO coated separator, respectively.

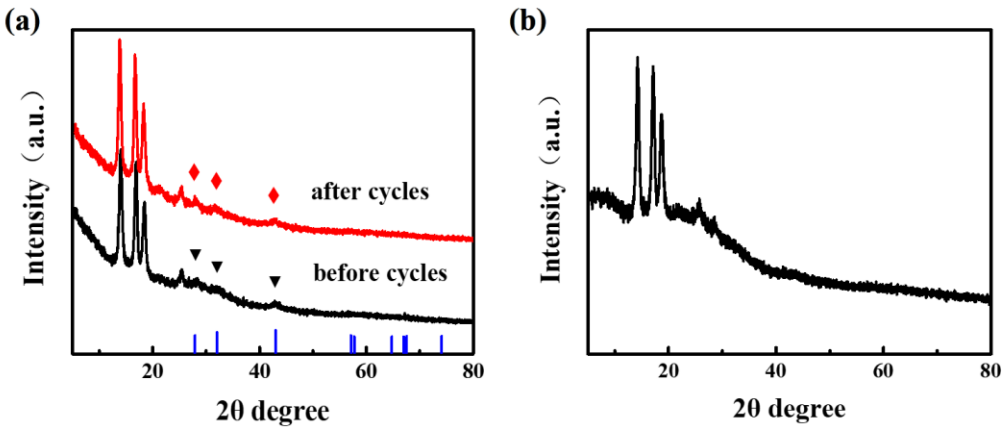


**Fig. S10** (a) XRD patterns of MoP/rGO modified separator before and after cycles; (b) XRD patterns of Celgard separator.

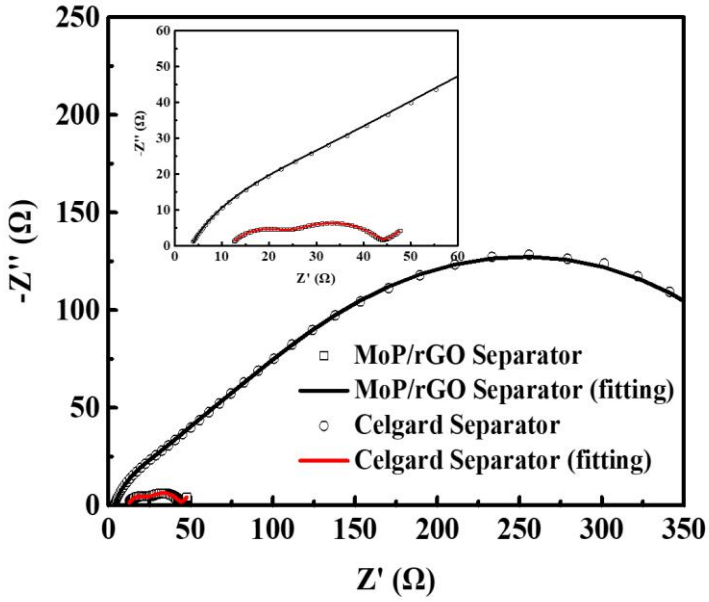


**Fig. S11** The electrochemical impedance spectra of cells with MoP/rGO coated separator and Celgard separator in full charge state after 100 cycles.

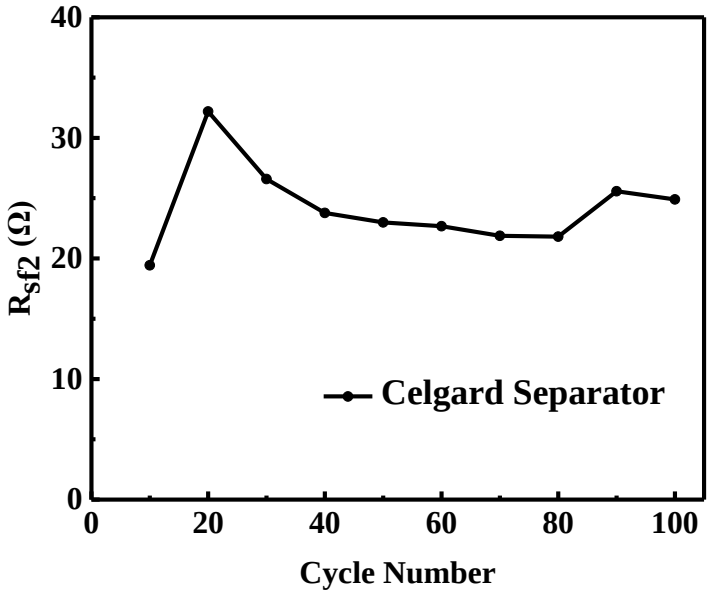


**Fig. S12** Interface resistance of $R_{sf2}$ of cell with Celgard Separator in full charged states for 100 cycles.

**Table S1** Comparison of performance of Li-S batteries with different interlayers

| Interlayers | Interlayers mass loading (mg cm$^{-2}$) | Sulfur mass loading (mg cm$^{-2}$) | Cathode (Sulfur content) | Electrochemical performance | | | |
|---|---|---|---|---|---|---|---|
| | | | | Rate | Initial Capacity (mAh g$^{-1}$) | Cycles | Capacity decay rate |
| MoP/rGO | 0.35~0.45 | 3.6 ~ 4 | CNT/S (77%) | 0.1 C | 1125 | 100 | 0.15% |
| | | | | 0.5 C | 880 | 300 | 0.045% |
| $Li_4Ti_5O_{12}$ / graphene | 0.346 | 1.0 ~ 1.2 | CNT/S 60% | 1 C | 813 | 500 | 0.029% |
| Boron-rGO | 0.2~0.3 | 1.5 | CNT/S (56%) | 0.1 C | 1227 | 300 | 0.153% |
| $TiO_2$ /graphene | 0.13 | 1.2 | CNT/S (82%) | 0.5 C | 802 | 250 | 0.072% |
| $TiO_2$ /carbon | 0.2 | 2 | C/S (60%) | 0.5 C | 920 | 200 | 0.087% |
| $MoS_2$ | N/A | N/A | C/S (65%) | 0.5 C | 808 | 600 | 0.083% |
| MWCNTs/ NCQDs | 0.15 | 1.3 ~ 1.5 | C/S (60%) | 0.5 C | 1330 | 500 | 0.1% |
| Black P | 0.4 | 1.5 ~ 2 | C/S (66%) | 0.5 C | 930 | 100 | 0.14% |
| GO | 0.12 | 1 ~ 1.5 | CNT/S (63%) | 0.1 C | 920 | 100 | 0.23% |

Reference:


[S1] Y. Zhao, M. Liu, W. Lv, Y. B. He, C. Wang, Q. B. Yun, B. H. Li, F. Y. Kang and Q. H. Yang, Nano Energy, 2016, 30, 1–8.

[S2] F. Wu, J. Qian, R. J. Chen, Y. S. Ye, Z. G. Sun, Y. Xing and L. Li, J. Mater. Chem. A, 2016, 4, 17033-17041.

[S3] Z. B. Xiao, Z. Yang, L. Wang, H. G. Nie, M. E. Zhong, Q. Q. Lai, X. J. Xu, L. J. Zhang and S. M. Huang, Adv. Mater., 2015, 27, 2891–2898.

[S4] H. Y. Shao, W. K. Wang, H. Zhang, A. B. Wang, X. N. Chen and Y. Q. Huang, Journal of Power Sources, 2018, 378, 537－545.

[S5] Z. A. Ghazi, X. He, A. M. Khattak, N. A. Khan, B. Liang, A. Iqbal, J. X. Wang, H. S. Sin, L. S. Li and Z. Y. Tang, Adv. Mater., 2017, 29, 1606817.

[S6] Y. Pang, J. S. Wei, Y. G. Wang and Y. Y. Xia, Adv. Energy Mater., 2018, 1702288.

[S7] J. Sun, Y. Sun, M. Pasta, G. Zhou, Y. Li, W. Liu and F. Xiong, Y. Cui, Adv. Mater., 2016, 28, 9797.

[S8] J. Huang, T. Zhuang, Q. Zhang, H. Peng, C. Chen and F. Wei, ACS Nano, 2015, 9, 3002.